

A quantum bouncing ball

Julio Gea-Banacloche

University of Arkansas, Fayetteville, Arkansas 72701

(Received 3 August 1998; accepted 21 January 1999)

The dynamics of a quantum wave packet bouncing on a hard surface under the influence of gravity are studied. This is a system that might be realized experimentally with cold atoms dropped onto an “atomic mirror.” The classical limit is discussed and interesting departures from classical behavior are pointed out and explained. © 1999 American Association of Physics Teachers.

I. INTRODUCTION

The solution of Schrödinger’s equation for a particle bouncing on a perfectly reflecting surface under the influence of gravity, that is, of a particle in the potential

$$V(z) = mgz, \quad z > 0 \\ = \infty, \quad z < 0, \quad (1)$$

is an intermediate-difficulty problem (exactly solvable using special functions) which is discussed in a number of textbooks.^{1,2} Sakurai,² for instance, uses it as an example of a system where the Wentzel-Kramers-Brillouin approximation gives an excellent approximation to the spectrum. The problem has also been treated in a number of pedagogical articles over the years in the pages of the American Journal of Physics: see, for instance, Refs. 3–5. It was given the name “The quantum bouncer” by Gibbs,⁴ who also discussed a two-dimensional extension, to a particle rolling down an inclined plane. (A more complicated kind of “quantum bouncer” is obtained when the mirror at the bottom is allowed to move; such a system may exhibit chaos in the classical limit, as discussed in Ref. 6.)

In recent years, the development of techniques to cool and manipulate atoms with high precision has made the simple quantum bouncer experimentally realizable.⁷ The reflecting surface is provided by a piece of glass “coated” with the evanescent field of a laser undergoing total internal reflection on the other side⁸ (a magnetic mirror can also be used).⁹ The atoms are dropped onto this surface from a small height, typically a few millimeters. A number of interesting precision measurements can be carried out in this way, including a determination of the van der Waals force between the atom and the glass.¹⁰ Although for most of these experiments the atoms energies are such that they behave essentially as classical particles, there is at least one experiment in which the (quantum) interference between parts of the wave packet reflected at different times was observed.¹¹ This may be regarded as a sort of first step toward a “matter wave cavity.”

This paper presents a study of the dynamics of a bouncing wave packet, initially Gaussian in shape, in the potential (1). Apart from its relevance to possible future experiments of the type described above, the problem is very interesting from a pedagogical standpoint, as it showcases some of the differences between classical and quantum dynamics. The classical motion is periodic (since no energy dissipation is assumed to take place), repeating itself indefinitely, but the quantum motion is aperiodic, and exhibits interesting collapses and revivals of the oscillations, similar to those observed in many other quantum systems. In spite of this, there is a clear correspondence between the classical and quantum

limits, and the use of a quasiclassical perspective allows one to derive some very useful results for the quantum problem as well.

The results reported here run the gamut from exact analytical expressions, to approximate ones, to fully numerical calculations. Impossible to present here, but available to anybody interested, is a movie that was generated showing the time evolution of the wave packet for some of the parameters discussed in the text. It can be downloaded from the following URL: http://www.uark.edu/misc/julio/bouncing_ball/bouncing_ball.html.

II. SOLUTION OF THE TIME-INDEPENDENT PROBLEM—SCALING

The time-dependent Schrödinger equation for the potential (1) reads

$$-\frac{\hbar^2}{2m} \frac{\partial^2 \Psi}{\partial z^2} + mgz \Psi = i\hbar \frac{\partial \Psi}{\partial t}, \quad (2)$$

with the boundary condition

$$\Psi(0, t) = 0 \quad (3)$$

at $z=0$. The solution will proceed via the usual expansion in the basis of energy eigenfunctions:

$$\Psi(z, t) = \sum_{n=1}^{\infty} C_n e^{-iE_n t/\hbar} \psi_n(z), \quad (4)$$

where the coefficients C_n are determined from the initial condition $\Psi(z, 0)$, and the eigenfunctions $\psi_n(z)$ are the solutions of

$$-\frac{\hbar^2}{2m} \frac{d^2 \psi_n}{dz^2} + mgz \psi_n = E_n \psi_n, \quad (5)$$

with the boundary condition

$$\psi_n(0) = 0. \quad (6)$$

To better exhibit the solution of (5), it is convenient to rescale the position and energy variables as follows: Introducing the characteristic “gravitational length” l_g defined as

$$l_g = \left(\frac{\hbar^2}{2gm^2} \right)^{1/3}, \quad (7)$$

let $z' = z/l_g$ and $E' = E/(mgl_g)$, or

$$E' = E \left(\frac{2}{\hbar^2 m g^2} \right)^{1/3}. \quad (8)$$

In these variables, Eq. (4) becomes

$$\frac{d^2\psi_n}{dz'^2} - (z' - E'_n)\psi_n = 0. \quad (9)$$

The solution to Eq. (9) is given by an Airy function, Ai or Bi, of the variable $z' - E'_n$.¹² Since the function Bi goes to infinity as its argument grows, it is not acceptable for this problem, where z is not bounded from above. The boundary condition (6) then means that E_n must be chosen so that $\text{Ai}(-E'_n) = 0$. If one denotes the zeros of the Airy function by $-z_n$, with $n = 1, 2, \dots$, and $z_n > 0$, one finds the solutions

$$E'_n = z_n, \quad (10a)$$

$$\psi_n(z') = \mathcal{N}_n \text{Ai}(z' - z_n), \quad (10b)$$

where \mathcal{N}_n is an appropriate normalization factor.

In what follows the primes on the energy and position variables will be dropped, and it will be understood that they are measured in the units introduced in Eqs. (7) and (8) above. It is also convenient to scale the time variable appearing in Eqs. (2) and (3). The natural time scale is $t_g = \hbar/(mgl_g)$, that is,

$$t_g = \left(\frac{2\hbar}{mg^2} \right)^{1/3}, \quad (11)$$

and from now on the time will be understood to be really $t' = t/t_g$.

For reference, for a Cs atom one finds $l_g = 0.226 \mu\text{m}$, a characteristic energy $mgl_g = 3.06 \times 10^{-12} \text{ eV}$ (corresponding to a temperature of about $4 \times 10^{-8} \text{ K}$), and a characteristic time $t_g = 0.22 \text{ ms}$, whereas for the much lighter Na atom one finds $l_g = 0.727 \mu\text{m}$, $mgl_g = 1.7 \times 10^{-12} \text{ eV}$ (a temperature of about $2 \times 10^{-8} \text{ K}$), and a characteristic time $t_g = 0.39 \text{ ms}$.

It is somewhat remarkable that all the eigenfunctions for this problem are ‘‘pieces’’ of the same function, the Airy function Ai, shifted in each case so that it has a zero at $z = 0$, and with the $z < 0$ part truncated. The first few (normalized) eigenfunctions are plotted in Fig. 1, along a horizontal axis. Like all stationary states, they have the characteristics of standing waves. Note how the wavelength of the oscillations decreases toward the bottom, in accordance with the de Broglie relationship $\lambda = h/mv$, since the speed of the classical particle is greater there. The higher-order wave functions correspond to the particle being ‘‘dropped’’ from progressively greater heights.

Exact analytical expressions for the zeros z_n and the normalization factors \mathcal{N}_n are not available, but good approximations can be given, especially for large n (which corresponds to the ‘‘quasiclassical’’ case to be discussed in this paper). For the zeros, one has

$$z_n \approx \left[\frac{3\pi}{2} \left(n - \frac{1}{4} \right) \right]^{2/3}. \quad (12)$$

These are also the angular frequencies of the time-dependent problem (4) when the scaled time t' is used. A very important difference with the simple harmonic oscillator is that these frequencies are not evenly spaced; that is, the difference $z_{n+1} - z_n$ depends on n . This means that the quantum motion is not, in general, periodic, even though the classical motion is. This will be explored in much greater detail in the following sections.

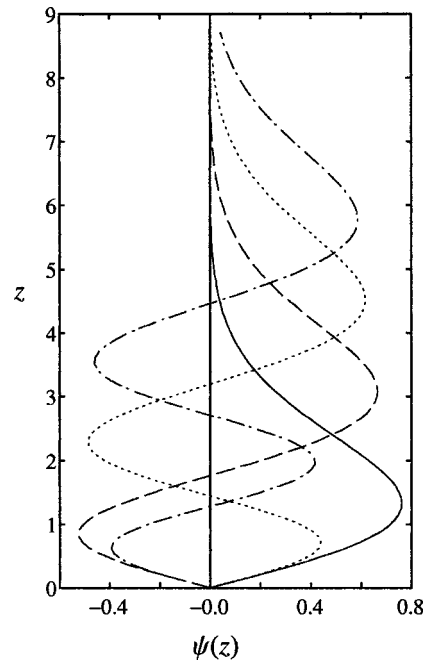


Fig. 1. The first four normalized eigenfunctions $\psi_n(z)$ of a particle in the potential (1) are plotted on the horizontal axis. Solid line: $n=1$ (ground state). Dashed line: $n=2$. Dotted line: $n=3$. Dash-dotted line $n=4$.

For the normalization factors \mathcal{N}_n , I have not been able to find even approximate expressions in the literature. Clearly, what is needed is

$$\mathcal{N}_n = \left[\int_0^\infty \text{Ai}^2(z - z_n) dz \right]^{-1/2}. \quad (13)$$

For large n , this expression may be manipulated somewhat using the asymptotic expansion of the Airy function. A little guesswork then yields the following, surprisingly accurate (for large n) expression:

$$\mathcal{N}_n \approx \left(\frac{\pi}{\sqrt{z_n}} \right)^{1/2} \approx \left[\frac{2\pi^2}{3(n-1/4)} \right]^{1/6}. \quad (14)$$

For $n=5$ the difference between the right-hand sides of (13) and (14) is only 0.0002, or 0.02%, and it improves as n increases. The details of the ‘‘derivation’’ of Eq. (14) are provided in the Appendix, in case they might inspire somebody to find a better approximation.

Last, for the full time-dependent solution (4) one needs the expansion coefficients C_n , which depend on the initial condition. For this paper I will assume an initial condition of the form of a Gaussian wave packet with a width σ and localized at a height z_0 above the ‘‘floor,’’ with zero initial momentum. That is, the particle is ‘‘dropped’’ from a height z_0 and bounces on thereafter. As long as $\sigma \ll z_0$, the following form will be, to a good approximation, normalized to unity in the $z=0$ to infinity range:

$$\Psi(z, 0) = \left(\frac{2}{\pi\sigma^2} \right)^{1/4} e^{-(z-z_0)^2/\sigma^2}. \quad (15)$$

For such a wave function the spread in position $\Delta z = \sigma/2$, so σ can be thought of as the ‘‘full width’’ of the wave packet.

The coefficients C_n are then given by

$$C_n = \mathcal{N}_n \left(\frac{2}{\pi \sigma^2} \right)^{1/4} \int_0^\infty \text{Ai}(z - z_n) e^{-(z - z_0)^2 / \sigma^2} dz. \quad (16)$$

Approximate expressions for the C_n can be calculated from (16) by using the following representation of the Airy function:

$$\text{Ai}(z) = \frac{1}{\pi} \int_0^\infty \cos \left(\frac{t^3}{3} + zt \right) dt. \quad (17)$$

Substituting (17) in (16) and carrying out the integration with respect to z (extending the lower limit to $-\infty$) yields

$$C_n \approx \mathcal{N}_n \left(\frac{2}{\pi \sigma^2} \right)^{1/4} \frac{\sigma}{\sqrt{\pi}} \int_0^\infty e^{-t^2 \sigma^2 / 4} \cos \left(\frac{t^3}{3} + (z_0 - z_n)t \right) dt. \quad (18)$$

Now, if σ is sufficiently large, meaning that the wave packet is initially a few times l_g in width, one can simplify Eq. (18) by expanding the t^3 term, since the exponential will ensure that t is never too large. The resulting integrals can all be evaluated exactly. Keeping only terms through t^3 yields

$$C_n \approx \mathcal{N}_n \left(\frac{2}{\pi \sigma^2} \right)^{1/4} \left(1 - 4 \frac{z_0 - z_n}{\sigma^4} + \frac{8}{3} \frac{(z_0 - z_n)^3}{\sigma^6} \right) \times e^{-(z_0 - z_n)^2 / \sigma^2}. \quad (19)$$

This is accurate to about 1% for $z_0 = 10$, $\sigma = 3$, and to about 10% for $z_0 = 10$, $\sigma = 2$. For sufficiently large values of σ and z_0 , the whole term in large parentheses can be replaced by 1.

The main usefulness of Eq. (19) is that, in conjunction with Eq. (12), it allows one to estimate how many wave functions need to be included in an approximate evaluation of the infinite sum (4), for given initial conditions. This is discussed further in the subsequent sections.

Although the case where $\sigma < 1$ (that is, $\Delta z < l_g$) will not be considered here, a few words about it may be in order. Since l_g is the approximate width of the ground state, it is also the length scale for which the product $\Delta z \Delta p$ is close to the minimum value allowed by the uncertainty principle for this problem. This means that decreasing Δz beyond this value will lead to a wave packet with a large momentum spread. For such a wave packet it is harder to get an intuitive feeling for what the quasiclassical limit should look like; in particular, if the momentum spread is large, the notion that the particle is being ‘‘dropped’’ with near zero momentum becomes untenable. For this reason, only wave packets with $\sigma > 1$ will be considered here.

III. THE CLASSICAL PROBLEM AND THE QUASICLASSICAL LIMIT

If the scalings introduced in Sec. II are applied to the classical equation of motion $d^2z/dt^2 = -g$, the result is, in effect, equivalent to setting the acceleration of gravity g equal to 2. The classical motion of a particle dropped from a height z_0 is simply characterized by a period T , equal to twice the time needed to reach the ground, which for $g = 2$ is simply

$$T = 2 \sqrt{z_0}. \quad (20)$$

Then one has

$$z(t) = 4z_0 \left[\frac{1}{4} - \left(\frac{t}{T} - n \right)^2 \right], \quad nT \leq t - \frac{T}{2} \leq (n+1)T, \quad n = 0, 1, \dots \quad (21)$$

This periodic motion can be expanded in a Fourier series,

$$z(t) = \sum_{p=-\infty}^{\infty} A_p e^{-2p\pi i t / T}, \quad (22)$$

with coefficients

$$A_p = \frac{1}{T} \int_0^T z(t) e^{-2p\pi i t / T} dt = (-1)^p \frac{2z_0}{p^2 \pi^2}, \quad p \neq 0 \\ = \frac{2}{3} z_0, \quad p = 0. \quad (23)$$

This Fourier series expansion actually applies, with small modifications, to all the possible initial conditions for this problem, including the cases when the particle is initially thrown upwards or downwards, provided z_0 is taken to be not the initial, but the maximum height; when scaled by z_0 and T , the trajectories corresponding to different initial conditions are, in fact, all identical except for a shift in the origin of time, which can be accounted for by shifting the phases of the coefficients A_p .

The result (21) for the classical problem may be compared to the corresponding time-dependent expectation value of the position operator z for the quantum problem, calculated from the wave function (4). Using (10a) one finds, in the scaled variables,

$$\langle z(t) \rangle = \sum_{n,m=1}^{\infty} C_n C_m^* \langle m|z|n \rangle e^{-i(z_n - z_m)t}, \quad (24)$$

where the matrix elements $\langle m|z|n \rangle$ are given by

$$\langle m|z|n \rangle = \mathcal{N}_n \mathcal{N}_m \int_0^\infty z \text{Ai}(z - z_n) \text{Ai}(z - z_m) dz. \quad (25)$$

To see how, and in what limit, the classical result (22) follows from (24), consider first the energy differences $z_n - z_m$ appearing in (24). One expects the classical limit to hold when the energies are large, and hence when n and m are large. Specifically, for a given z_0 one expects, from Eq. (19), that the values of z_n, z_m contributing to the sum (24) will all be within a range of a few times σ from z_0 . One can define a number n_0 as the order of the zero of the Airy function Ai which is closest to $-z_0$. By the approximate expression (12), one finds

$$n_0 \approx \frac{2z_0^{3/2}}{3\pi} + \frac{1}{4}, \quad (26)$$

where it is understood that n_0 is, in fact, the integer closest to the real number on the right-hand side of (26). If this number is large, the difference between it and n_0 will be negligible, relatively speaking.

One can then expand the frequencies z_n given by Eq. (12) around n_0 : that is, set $z_n = z_{n_0 + (n - n_0)}$ and expand in $n - n_0$. The three lowest-order terms are

$$z_n \approx z_{n_0} + \frac{\pi}{\sqrt{z_{n_0}}}(n - n_0) - \frac{\pi^2}{4z_{n_0}^2}(n - n_0)^2$$

$$\approx z_0 + \frac{\pi}{\sqrt{z_0}}(n - n_0) - \frac{\pi^2}{4z_0^2}(n - n_0)^2. \quad (27)$$

The range of values of n , Δn , appearing in (27) can be estimated as follows. From the linear term in (27), one can see that $\Delta n \sim \sqrt{z_0} \Delta z_n$. From Eq. (19), the range of z_n , Δz_n , can be expected to be of the order of a few times σ around z_0 . Thus one expects

$$\Delta n \sim \sigma \sqrt{z_0}. \quad (28)$$

With this, the order of magnitude of the three terms on the right-hand side of (27) is seen to be

$$z_0, \sigma, \frac{\sigma^2}{z_0}. \quad (29)$$

The condition for the quadratic term to be negligible versus the linear one is, therefore,

$$\sigma \ll z_0; \quad (30)$$

this is, a well-localized wave packet, which is just what one would expect for the classical limit to hold. Note also that (28) and (26) imply that, when the condition (30) holds, the range of important values of n , Δn , would be much smaller than n_0 itself.

Assuming that (30) holds and neglecting the quadratic term in (27) for the moment (its effects will be discussed at great length in Sec. IV), one can see that the frequency differences $z_n - z_m$ appearing in (24) are approximately given by

$$z_n - z_m \approx \frac{\pi}{\sqrt{z_0}}(n - m) = \frac{2\pi}{T}(n - m), \quad (31)$$

where T is the classical period, given by Eq. (20). This shows that, indeed, in this limit the quantum expectation value (24) has the same periodic time dependence as the classical position (22). The sum in (24) can be rearranged, in this limit, to read

$$\langle z(t) \rangle = \sum_{p=-\infty}^{\infty} \left(\sum_{m=\max(1, 1-p)}^{\infty} C_{m+p} C_m^* \langle m|z|m+p \rangle \right) \times e^{-2p\pi i t/T}. \quad (32)$$

One would expect that, in the appropriate quasiclassical limit ($z_0 \gg \sigma \gg 1$), the term in parentheses in (32) would reduce to the appropriate A_p coefficient of Eq. (22), and it seems *a priori* that there are a number of ways in which this could be accomplished.

What I have found (numerically) for this problem is that the matrix element $\langle m|z|m+p \rangle$ is, in fact, given by a very simple result strongly reminiscent of the classical result (23):

$$\langle m|z|m+p \rangle = (-1)^p \frac{2}{(z_m - z_{m+p})^2}, \quad p \neq 0$$

$$= \frac{2}{3z_m}, \quad p = 0. \quad (33)$$

Note how, in the limit when (31) holds, this reduces to

$$\langle m|z|m+p \rangle \approx A_p, \quad (34)$$

with the classical coefficients A_p given by Eq. (23) above.

It may be worth pointing out that Eq. (33) is a very non-trivial result, and, in fact, I was only able to guess at it by considering the classical limit, as indicated above. Using Eqs. (25) and (13) to recast it in terms of the Airy function, it reads

$$\int_0^{\infty} z \text{Ai}(z - z_n) \text{Ai}(z - z_m) dz$$

$$= 2 \frac{(-1)^{n-m}}{(z_n - z_m)^2} \left[\int_0^{\infty} \text{Ai}^2(z - z_n) dz \int_0^{\infty} \text{Ai}^2(z - z_m) dz \right]^{1/2},$$

$$n \neq m, \quad (35a)$$

$$\int_0^{\infty} z \text{Ai}^2(z - z_n) dz = \frac{2}{3} z_n \int_0^{\infty} \text{Ai}^2(z - z_n) dz, \quad (35b)$$

where $-z_n$ and $-z_m$ are any of the zeros of the function $\text{Ai}(z)$. I have not been able to find either of these identities in the literature, and I have not been able to prove them analytically, either, but numerical calculations show them to be "exact" that is, true to an arbitrary precision, for arbitrary values of n and m .

The classical limit now follows fairly easily. Use of (34) in (32) yields

$$\langle z(t) \rangle = \sum_{p=-\infty}^{\infty} \left(\sum_{m=\max(1, 1-p)}^{\infty} C_{m+p} C_m^* \right) A_p e^{-2p\pi i t/T}. \quad (36)$$

For the particular initial condition considered here, one may use Eq. (19) for the coefficients C_m , with the term in the large parentheses replaced by 1 in the classical limit. Also, one may use the linear term in (27) to express $z_n - z_0$ in terms of $n - n_0$, and note that, since the resulting Gaussian functions of m are sharply peaked around n_0 and $n_0 - p$ with $n_0 \gg 1$, there is no harm in formally extending the sum range to $-\infty$ from below. Using also the asymptotic form (14) of the coefficients \mathcal{N}_n , with $z_n \approx z_0$, finally yields

$$\sum_{m=\max(1, 1-p)}^{\infty} C_{m+p} C_m^*$$

$$\approx \sqrt{\frac{2\pi}{\sigma^2 z_0}} \sum_{m=-\infty}^{\infty} e^{-\pi^2 [(m - n_0)^2 + (m + p - n_0)^2] / \sigma^2 z_0}$$

$$\approx e^{-\pi^2 p^2 / 2\sigma^2 z_0}. \quad (37)$$

In the last step, the sum over m has been approximated by an integral. The full expression is therefore

$$\langle z(t) \rangle \approx \sum_{p=-\infty}^{\infty} e^{-\pi^2 p^2 / 2\sigma^2 z_0} A_p e^{-2p\pi i t/T}. \quad (38)$$

When compared to (22) one can see that the high temporal frequencies (large p) in the quantum expectation value may be suppressed, because of averaging over the wave packet's width. In any event, the classical result (22) is clearly recovered in the limit of large z_0 .

For values of z_0 that are not too large, however, the quantum result may look substantially different from the classical one as a function of time, as Fig. 2 illustrates for the cases $z_0 = 10$, $\sigma = 2(a)$ and $z_0 = 20$, $\sigma = 3$. (b) The particle's first few bounces are clearly well defined, but after a while the

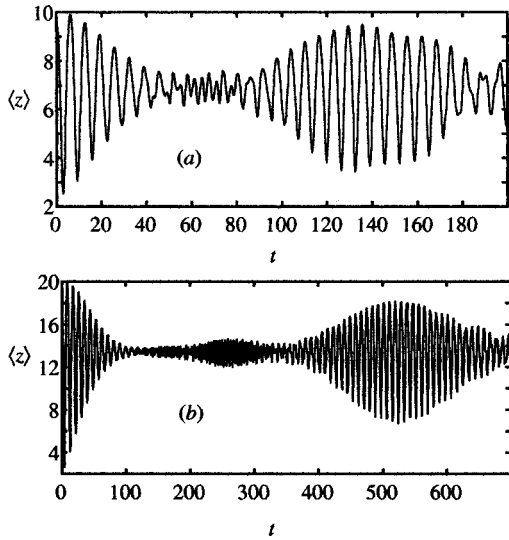


Fig. 2. Expectation value of the position as a function of time for a wave packet with (a) $z_0=10$, $\sigma=2$, and (b) $z_0=20$, $\sigma=3$. Time is in units of t_g , length is in units of l_g .

bounces cease and the expectation value of z remains very close to the time average of the classical trajectory, $2z_0/3$ [Eq. (23)]. Further, after yet some more time the oscillations revive and the particle begins to bounce again.

This collapse and revival of classically periodic motion is a well-known feature of many quantum systems.¹³ It is clearly not predicted by (38); in fact, it can be explained, at least in its most salient features, by a careful study of the quadratic term in Eq. (27), which was neglected in going from (24) to (32). This is discussed in detail in Sec. IV.

IV. QUANTUM DYNAMICS: COLLAPSES AND REVIVALS

When the quadratic term in (27) is kept in expression (24) for the quantum expectation value, the argument of the exponential becomes

$$-i(z_n - z_m) \approx -i \frac{2\pi t}{T} (n - m) + i \frac{4\pi^2 t}{T^4} [(n - n_0)^2 - (m - n_0)^2]. \quad (39)$$

Clearly, for sufficiently large times the last term in (39) will not be negligible, and it may cause the various Fourier components in Eq. (24) to drift out of phase and cancel each other out. The only surviving terms will be those with $n = m$, i.e., the ones giving the (classical) time average. This leads to the collapse of the oscillations seen in Fig. 2.

The size of the second term in (39) depends on $n - m$, that is, on the Fourier component, or oscillation frequency, one is looking at. Higher frequencies dephase faster. The collapse that is most readily apparent in Fig. 2 is that of the oscillations at the slowest nonvanishing frequency, $2\pi/T$, corresponding to $n = m \pm 1$. For this case, the second term in (39) reads

$$i \frac{4\pi^2 t}{T^4} [\pm 2(m - n_0) + 1] \sim i \frac{8\pi^2 t}{T^4} \Delta n \sim i 4\pi^2 \frac{\sigma}{T^3} t \quad (40)$$

[using (28) for an estimate of Δn]. The collapse time can be estimated then from the time it takes this term to be of the order of $i\pi$.

It is also possible, and instructive, to understand the collapse through purely quasiclassical arguments. For this, imagine that the wave packet with a width σ represents an ensemble of particles that are all dropped simultaneously from slightly different heights. Since the frequency of the bouncing motion depends on the height [Eq. (20)], eventually all these imaginary particles get out of phase. Specifically, as Eq. (20) implies $\omega = \pi/\sqrt{z_0}$, $\delta\omega = \pi\delta z_0/2z_0^{3/2}$, and setting $\delta z_0 \sim \sigma$ one finds the different parts of the wave packet should get out of phase after a time T_c of the order of $\delta\omega T_c \sim \pi$, or

$$T_c \sim \frac{2z_0^{3/2}}{\sigma} = \frac{T^3}{4\sigma}. \quad (41)$$

Indeed, the collapse time seen in Fig. 2, as well as those observed in other numerical calculations, agrees very well with the estimate (41). This is the time when the lower half of the wave packet has gotten approximately half a cycle ahead of the upper half. Clearly, this also agrees with the quantum-mechanically derived estimate in (40) above.

Unlike the collapse, the revival of the oscillations, which is also apparent in Fig. 2, has no simple quasiclassical explanation, and is best seen as a purely quantum phenomenon, ultimately due to the discreteness of the energy levels of the bouncing particle. The main point is that n and m in Eq. (39) above are integers, which means that at some special time t such that $4\pi t/T^4 = 1$ the last term in (39) will be a multiple of $i\pi$ for all values of n and m , and no dephasing will result. (Why it suffices to have a multiple of π , and not 2π , will be explained below.)

Consider then the ‘‘revival time’’ T_r defined by

$$T_r = \frac{T^4}{4\pi} = \frac{4z_0^2}{\pi} \quad (42)$$

and a time nearby, $t = t_r + \delta t$. The value of the last term in (39) is at that time

$$i \frac{4\pi^2 t}{T^4} [(n - n_0)^2 - (m - n_0)^2] = i\pi(n - m)(n + m - 2n_0) + i \frac{4\pi^2 \delta t}{T^4} (n - m)(n + m - 2n_0). \quad (43)$$

The size of the second term in this expression can be estimated, as before, to be, for the slowest nonvanishing frequency ($n = m \pm 1$), of the order of $\delta t/T_c$, where T_c is the collapse time. For $\delta t \ll T_c$, it could be neglected. Thus, for a range of times of the order of T_c around the revival time T_r , the second term in (39) will be, to a fair approximation, an integer multiple of $i\pi$, of the form $i\pi(n - m)(n + m - 2n_0)$.

The factor $(n - m)(n + m - 2n_0)$ has the same parity (odd or even) as $n - m$ itself. When $n - m$ is odd, an odd multiple of π can be pulled out of the first term in (39) by shifting the time t by half a period, $T/2$. Thus around the revival time one could approximate (39) by

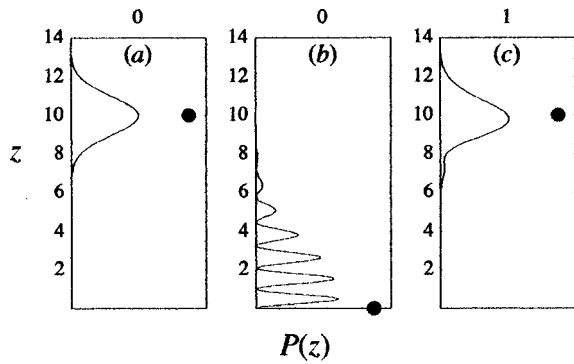


Fig. 3. The first bounce for a wave packet with $z_0=10$, $\sigma=2$ [as in Fig. 2(a)]. The closed circle represents the position of the corresponding classical particle. The quantum probability distribution $P(z)=|\Psi|^2$ is plotted along the horizontal axis. Lengths are in units of l_g . The number at the top of each frame keeps track of the number of classical bounces up to that time, and changes immediately after the classical particle hits the floor.

$$\begin{aligned}
 -i(z_n - z_m)t &\approx -i \frac{2\pi t}{T} (n - m) \\
 &+ i \frac{4\pi^2 t}{T^4} [(n - n_0)^2 - (m - n_0)^2] \\
 &\approx -i \frac{2\pi(t - T/2)}{T} (n - m) \\
 &+ i\pi(n - m)(n + m + 1 - 2n_0) \quad (44)
 \end{aligned}$$

and the last term in this expression is always an even multiple of $i\pi$. Hence, around the revival time one sees the quantum particle bouncing again, only *half a period out of phase* with the classical motion.

For the example in Fig. 2(a), for instance, the period is $T=6.32$, and the revival time is $T_r=127$ (note that, unlike the collapse time, the revival time is independent of the width σ of the initial wave packet, although the overall duration and fidelity of the revival does depend on σ). The peak of the oscillation around $t=129.3$, near the revival maximum, corresponds to $129.3/6.32 \approx 20.5$ periods; that is, it would have been a minimum of the classical motion. [This is also true for Fig. 2(b), provided one uses the more nearly correct value $2\sqrt{z_{n_0}}$, rather than $2\sqrt{z_0}$, for the period of the quantum motion, as it makes a difference when calculating the dephasing over the very long times shown in the figure; cf. Eq. (27).]

The dephasing is also clearly seen in the animation available at http://www.uark.edu/misc/julio/bouncing_ball/bouncing_ball.html. Figures 3 and 4 show several frames from this animation, where the quantum probability distribution is plotted along the horizontal axis, and a circle on the right represents the position of the classical particle. The number at the top is the number of the classical bounce. Figure 3 shows the first bounce: 3(a) is the initial state, 3(b) is the particle just reaching the floor (note the interference, in the quantum-mechanical wave function, between the part of the wave packet going down and the part being reflected up; see Ref. 14 for a recent, pedagogical discussion of this type of interference), and 3(c) is half a period later, the top of the first bounce.

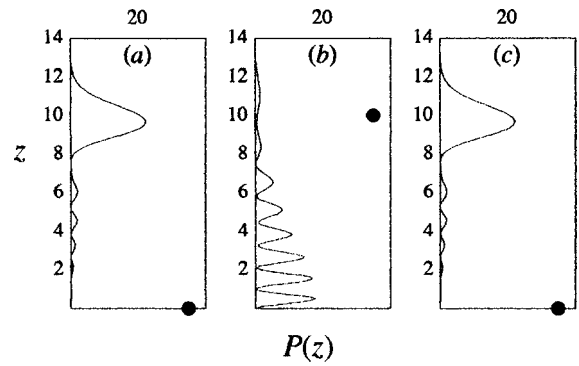


Fig. 4. Same as Fig. 2, but around the revival time $t=129.3$ (20 classical bounces).

Figure 4 corresponds to the revival region. Figure 4(a) shows the classical particle just rising from the floor after 20 bounces; the π radians dephasing with the quantum particle is evident. Figure 4(b) shows it at the top of the 20th bounce, at the time $t=20.5T$ calculated earlier; and Fig. 4(c) again at the bottom. The figures show that the revival of the initial wave function isn't quite perfect, but for these parameters (a fairly narrow initial wave packet) it is actually pretty good.

The behavior of the wave function in the collapse region is harder to visualize from still frames, and generally harder to interpret. A naive interpretation of the expectation value plots shown in Fig. 2 might suggest that the particle is just hovering in mid-air! In fact, at times, as in Fig. 5(a), the wave packet appears to be fairly cleanly split into two pieces, moving in opposite directions. They interfere constructively around $z=2z_0/3$ [Fig. 5(b)]. At other times the wave packet is more uniformly spread out and resembles more a standing wave [Fig. 5(c)].

V. CONCLUSIONS

The dynamics of the quantum bouncing ball are an interesting problem which shows, once more, that the classical limit of a quantum mechanical system is not necessarily trivial. The collapse of the oscillations admits of a simple quasiclassical explanation, whereas the revivals are purely quantum, a consequence of the discrete energy spectrum of the problem. In the classical limit, as $z_0 \rightarrow \infty$, both the collapse and revival times go to infinity, but they do so over different scales (the revival goes away much faster). Also,

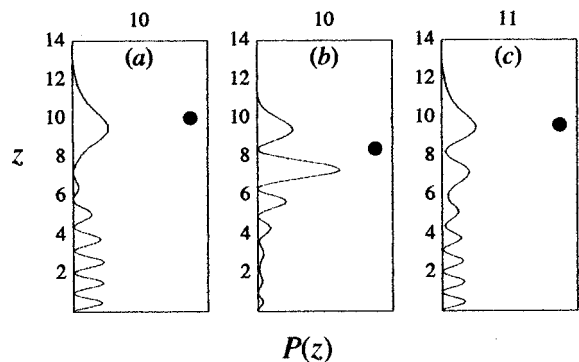


Fig. 5. Same as Fig. 2, but around the middle of the collapse region ($t \sim 63-70$).

although the quantum problem is intrinsically aperiodic, the correspondence between the Fourier coefficients of the classical motion and the matrix elements of the position operator [Eqs. (33) and (34)] is remarkable and instructive.

The revivals can also be interpreted as an interference phenomenon between the various parts of the wave packet which have bounced a different number of times. This suggests that they could be sensitive to the presence of any phase-shifting elements along the path of the bouncing ball, or to phase shifts experienced by the wave packet upon reflection on the surface. This is an interesting possibility which may be worth looking into.

The main problem in observing the effects described here experimentally are the very low energies required. The atoms would have to be very cold, on the order of tens of nanokelvins. While low, these temperatures are certainly not unreachable: Raman cooling of Cs to below 3 nK was already demonstrated three years ago.¹⁵ What may be harder is to cool and drop the atoms from a very small height (only a few microns) above the mirror. This is necessary if one wants to be able to observe a full collapse and revival, since the revival time scales as T^4 , which means that the number of bounces needed to observe a full revival goes as $T^3 \sim z_0^{3/2}$, and a number of atoms will inevitably be lost in each bounce. A possible way to increase the effective gravitational length l_g and relax this constraint somewhat might be to place the atoms in a strong electric or magnetic field that would provide a vertical constant force to partially compensate for gravity, in effect lowering the value of g .

A note on the numerical calculations: For many of the results reported here, and, in particular, to generate the animation, the commercial package MATHEMATICA was used on a personal computer (thanks are due to T. D. Snyder for help in making a cross-platform, browser-viewable version of the animation). For other calculations, the Airy function was computed using the numerical routines given in Ref. 16.

APPENDIX: APPROXIMATE EXPRESSION FOR THE NORMALIZATION FACTORS

Since all the eigenfunctions for this problem are pieces of the function $\text{Ai}(z)$, the difference between two consecutive normalization factors (13) is given by

$$\frac{1}{\mathcal{N}_{n+1}^2} - \frac{1}{\mathcal{N}_n^2} = \int_{-z_{n+1}}^{-z_n} \text{Ai}^2(z) dz. \quad (\text{A1})$$

For sufficiently large n , one may use the asymptotic form

$$\text{Ai}(z) \approx \frac{1}{\pi^{1/2}} \frac{1}{z^{1/4}} \cos\left(\frac{2}{3} z^{3/2} - \frac{\pi}{4}\right) \quad (\text{A2})$$

to evaluate the right-hand side of (A1) approximately. With the change of variable $u = (2/3)z^{3/2}$, and using the approximation (12) for the zeros z_n [which is consistent with the form (A2)], one obtains

$$\begin{aligned} \frac{1}{\mathcal{N}_{n+1}^2} - \frac{1}{\mathcal{N}_n^2} &\approx \frac{1}{\pi} \int_{(n-1/4)\pi}^{(n+3/4)\pi} \frac{1}{(3u/2)^{2/3}} \cos^2\left(u - \frac{\pi}{4}\right) du \\ &\approx \frac{1}{\pi} \left[\frac{3\pi}{2} \left(n - \frac{1}{4}\right) \right]^{-2/3} \int_{-\pi/2}^{\pi/2} \cos^2 u du \\ &= \frac{1}{2\pi} \left[\frac{3\pi}{2} \left(n - \frac{1}{4}\right) \right]^{-2/3}. \end{aligned} \quad (\text{A3})$$

One can then say that for large n ,

$$\frac{d}{dn} \frac{1}{\mathcal{N}_n^2} \approx \frac{1}{2\pi} \left[\frac{3\pi}{2} \left(n - \frac{1}{4}\right) \right]^{-2/3} \quad (\text{A4})$$

and integrate this formally with respect to n to get something like

$$\frac{1}{\mathcal{N}_n^2} \approx \frac{1}{\pi} \left[\frac{3\pi}{2} \left(n - \frac{1}{4}\right) \right]^{1/3} + C \approx \frac{\sqrt{z_n}}{n} + C \quad (\text{A5})$$

for some constant C . As it happens, numerical evaluation of (13) shows that the expression (A5) is basically accurate, with C a number smaller than 0.004 (for $n=1$) and decreasing steadily as n increases.

¹D. ter Haar, *Selected Problems in Quantum Mechanics* (Academic, New York, 1964), Sec. 1.24.

²J. J. Sakurai, *Modern Quantum Mechanics* (Benjamin/Cummings, Menlo Park, CA, 1985).

³P. W. Langhoff, "Schrödinger particle in a gravitational well," *Am. J. Phys.* **39**, 954–957 (1971).

⁴R. L. Gibbs, "The quantum bouncer," *Am. J. Phys.* **43**, 25–28 (1975).

⁵R. D. Desko and D. J. Bord, "The quantum bouncer revisited," *Am. J. Phys.* **51**, 82–85 (1983); D. A. Goodins and T. Szeredi, "The quantum bouncer by the path integral method," *ibid.* **59**, 924–930 (1991); S. Whinerray, "An energy representation approach to the quantum bouncer," *ibid.* **60**, 948–950 (1992).

⁶S. T. Dembiński, A. J. Makowski, and P. Pełowski, "Quantum bouncer with chaos," *Phys. Rev. Lett.* **70**, 1093–1096 (1993); see also S. T. Dembiński and L. Wolniewicz, "Remarks on solving the one-dimensional time-dependent Schrödinger equation on the interval $[0, \infty]$: The case of a quantum bouncer," *J. Phys. A* **29**, 349–355 (1996).

⁷See, for many references, J. P. Dowling and J. Gea-Banacloche, "Evanescence Light-Wave Atom Mirrors, Resonators, Waveguides, and Traps," *Adv. At. Mol., Opt. Phys.* **37**, 1–94 (1996).

⁸C. G. Aminoff, A. Steane, M. P. Bouyer, P. Desbiolles, J. Dalibard, and C. Cohen-Tannoudji, "Cesium atoms bouncing in a stable gravitational cavity," *Phys. Rev. Lett.* **71**, 3083–3086 (1993).

⁹T. M. Roach, H. Abele, M. G. Boshier, H. L. Grossman, K. P. Zetie, and E. A. Hinds, "Realization of a magnetic mirror for cold atoms," *Phys. Rev. Lett.* **75**, 629–632 (1995).

¹⁰A. Landragin, Y.-J. Courtois, G. Labeyrie, N. Vansteenkiste, C. I. Westbrook, and A. Aspect, "Measurement of the van der Waals force in an atomic mirror," *Phys. Rev. Lett.* **77**, 1464–1467 (1996).

¹¹P. Szriftgiser, D. Guéry-Odelin, M. Arndt, and J. Dalibard, "Atomic wave diffraction and interference using temporal slits," *Phys. Rev. Lett.* **77**, 4–7 (1996).

¹²M. Abramowitz and I. A. Stegun (eds.), *Handbook of Mathematical Functions* (Dover, New York, 1972), Sec. 10.4.

¹³See, for instance, N. B. Narozhny, J. J. Sánchez-Mondragón, and J. H. Eberly, "Coherence versus incoherence: Collapse and revival in a simple quantum model," *Phys. Rev. A* **23**, 236–247 (1981); J. Parker and C. R. Stroud, Jr., "Coherence and decay of Rydberg wave packets," *Phys. Rev. Lett.* **56**, 716–719 (1986).

¹⁴M. Andrews, "Wave packets bouncing off walls," *Am. J. Phys.* **66**, 252–254 (1998).

¹⁵J. Reichel, F. Bardou, M. Ben Dahan, E. Peik, S. Rand, C. Salomon, and C. Cohen-Tannoudji, "Raman cooling of cesium below 3 nK: New approach inspired by Lévy flight statistics," *Phys. Rev. Lett.* **75**, 4575–4578 (1995).

¹⁶W. H. Press, S. A. Teukolsky, W. T. Vetterling, and B. P. Flannery, *Numerical Recipes in C* (Cambridge U.P., Cambridge, 1992), 2nd ed., Sec. 6.7.